HORIZONTAL RADIATIVE FLUXES IN CLOUDS AT ABSORBING WAVELENGTHS

A. Marshak[†], A. B. Davis[††], L. Oreopoulos[†], and W. J. Wiscombe[†††]

Prepared for *Geophysical Research Letters* , October 5, 1998

Corresponding author: Alexander Marshak (marshak@climate.gsfc.nasa.gov)

Abstract

We discuss the effect of horizontal fluxes on the accuracy of a conventional plane-parallel radiative transfer calculation for a single pixel, known as the Independent Pixel Approximation (IPA) at absorbing wavelengths. Vertically integrated horizontal fluxes can be represented as a sum of three components; each component is the IPA accuracy on a pixel-by-pixel basis for reflectance, transmittance and absorptance, respectively. We show that IPA accuracy for reflectance always improves with more absorption, while the IPA accuracy for transmittance is less sensitive to the changes in absorption: with respect to the non-absorbing case, it may first deteriorate for weak absorption and then improve again for strongly absorbing wavelengths. IPA accuracy for absorptance always deteriorates with more absorption. As a result, vertically integrated horizontal fluxes, as a sum of IPA accuracies for reflectance, transmittance and absorptance, increase with more absorption. Finally, the question of correlations between horizontal fluxes, IPA uncertainties and radiative smoothing is addressed using wavenumber spectra of radiation fields reflected from or transmitted through fractal clouds.

[†] Joint Center for Earth Systems Technology,
University of Maryland Baltimore County,
1000 Hilltop Circle, Baltimore, MD 21250

[††] Los Alamos National Laboratory,
Space & Remote Sensing Science (NIS-2),
PO Box 1663 (MS-C323)
Los Alamos, NM 87545

[†††] NASA – Goddard Space Flight Center,
Climate & Radiation Branch (Code 913),
Greenbelt, MD 20771

1. Introduction

In order to correctly interpret radiation reflected from or transmitted through clouds and measured by satellites and ground-based radiometers or two aircraft flying above and below clouds, we need to better understand interactions between inhomogeneous clouds and solar radiation. The discrepancies between observed and model-predicted shortwave absorption (e.g., Cess et al., 1995, Wiscombe, 1995), between cloud optical depths estimated from satellites and ground measurements (Min and Harrison, 1996), between single scattering albedo retrieved from in situ radiation measurements and computed from measured droplet size distribution (Pincus et al., 1997), amongst other reasons, are strongly affected by cloud horizontal inhomogeneity.

Net horizontal photon transport (i. e., horizontal fluxes) are a direct consequence of the inhomogeneity in cloud structure. Horizontal fluxes and their effect on the accuracy of the pixel-by-pixel one-dimensional (1D) radiative transfer calculations has recently undergone close scrutiny for conservative scattering (Marshak et al., 1995a; Barker, 1996; Davis et al., 1997a, b, c; Chambers et al., 1997; Titov and Kasjanov, 1997; Titov, 1998; Zuidema and Evans, 1998). However, the properties and magnitude of horizontal fluxes in absorbing wavelengths are still poorly understood. As far as we are aware, only Ackerman and Cox (1981) and Titov (1998) briefly discussed correlations between horizontal fluxes at different wavelengths.

This paper partly fills this gap. We discuss here an intriguing question of whether the accuracy of the Independent Pixel Approximation (IPA), as a 1D radiative transfer approximation for each pixel, is better for transparent or absorbing wavelengths. The main original points to be addressed here are:

- dependence of net horizontal fluxes on single-scattering albedo;
- connection between pixel-by-pixel accuracy of the IPA and horizontal fluxes;
- radiative smoothing and horizontal fluxes in wavelengths with liquid water absorption.

2. Cloud Models and Numerical Radiative Transfer Tools

The key point of our cloud models is a scale-invariant horizontal distribution of cloud optical depth τ. We started with simple one- or two-dimensional (2D) "bounded cascade" models (Cahalan, 1994, Marshak et al., 1994) that simulate cloud inner structure with $\tau > 0$ for the whole domain. Then we supplemented this structure with gaps using a simple procedure that first linearly transforms τ and then sets negative values to zero (Marshak et al., 1998). Finally, we added cloud-top variability using a fractional Brownian motion (Mandelbrot, 1977).

We show results where we set mean optical depth $\langle\tau\rangle = 13$, mean geometrical thickness $\langle h\rangle = 300$ m, bounded cascade model with variance parameter $p = 0.3$ and scaling parameter $H = 1/3$ (Marshak et al., 1994). All these parameters are typical of marine stratocumulus (Cahalan et al., 1994). Pixel size was set to 25 m; a 10-step cascade model then yields outer scale $L = 25.6$ km. All results presented below are averaged over ten independent realizations of stochastic cloud models.

Both Henyey-Greenstein with asymmetry parameter $g = 0.85$ and C1 cloud (Deirmendjian, 1969) scattering phase functions were used. To study the dependence on single-scattering albedo ϖ_0, seven albedos were chosen for our simulations: 1.00, 0.999, 0.996, 0.99, 0.98, 0.95, 0.9 which cover the range currently calculated for pure liquid water clouds in the shortwave spectrum.

Two traditional numerical methods were chosen for radiative transfer calculations in the cloud models above. They are the Independent Pixel Approximation (IPA) and Monte Carlo (MC) simulation. While the later is the "exact statistical" solution (Marchuk et al., 1980) of the three-dimensional (3D) radiative transfer equation (see below) with periodic boundary conditions, the former is a plane-parallel solution applied on a pixel-by-pixel basis (Cahalan et al., 1994) and calculated using either a two-stream approximation (Lenoble, 1985), DISORT (Stamnes et al., 1988) or MC with very large horizontal pixel sizes.

3. Horizontal Flux and Its Components

To determine photon horizontal transport, we start with the radiative transfer equation (e.g., Lenoble, 1985)

$$\Omega \bullet \nabla I = -\sigma(x) I(x,\Omega) + \sigma(x)\varpi_0 \int_{4\pi} p(\Omega' \rightarrow \Omega) I(x,\Omega') d\Omega' \qquad (1)$$

where $I(x,\Omega)$ is a radiance at a point $x = (x,y,z)$ in direction $\Omega = (\Omega_x,\Omega_y,\Omega_z)$, $p(\Omega' \rightarrow \Omega)$ is the (normalized) scattering phase function, $\sigma(x)$ is extinction coefficient and, finally, ϖ_0 is a single-scattering albedo. If Eq. (1) is integrated term-by-term with respect to Ω (over 4π) and z (from cloud base, z_b, to cloud top, z_t), we get a relationship (Titov, 1998) between vertically integrated horizontal fluxes $H(x,y)$, column absorption $A(x,y)$, reflectance $R(x,y)$ and transmittance $T(x,y)$. In a simple case of $\sigma(x) \equiv \sigma(x)$, we have (Ackerman and Cox, 1981; Davis et al., 1997a; Marshak et al., 1998)

$$H(x) = \int_{z_b}^{z_t} \frac{\partial}{\partial x} \int_{4\pi} \Omega_x I(x,z;\Omega) d\Omega dz = -\int_{z_b}^{z_t} \frac{\partial}{\partial z} \int_{4\pi} \Omega_z I(x,z;\Omega) d\Omega dz - (1-\varpi_0)\sigma(x) \int_{z_b}^{z_t} \int_{4\pi} I(x,z;\Omega) d\Omega dz$$

The first term in the right-hand side of the above equation is the difference between two net fluxes at z_t and z_b, while the second one is column absorption. In other words,

$$H(x) = \{[1-R(x)] - [T(x)-0]\} - A(x), \quad 0 \le x \le L, \qquad (2)$$

i.e., vertically integrated horizontal fluxes $H(x)$ is determined as a difference between "true" column absorption $A(x)$ and its "apparent" counterpart, $1-R(x)-T(x)$.

Equation (2), however, does not say anything about computational accuracy if, instead of full 3D radiative transfer, a fast IPA is used. We know that IPA treats each pixel as an independent plane-parallel medium neglecting any net horizontal photon transport. In order to relate horizontal fluxes and pixel-by-pixel accuracy of the IPA, we substi ute unity in Eq. (2) by the sum of $R_{IPA}(x)$, $T_{IPA}(x)$ and $A_{IPA}(x)$. As a result, H is represented as a sum of three components,

$$H(x) = H_R(x) + H_T(x) + H_A(x). \qquad (3)$$

Each component in Eq. (3) is a pixel-by-pixel IPA error (or accuracy),

$$H_F(x) = F_{\mathrm{IPA}}(x) - F(x) \tag{4}$$

where F is either R, T or A. Since H_R, H_T and H_A are reflection, transmission, and absorption components of vertically integrated horizontal fluxes, we also will call them horizontal fluxes for photons reflected from cloud top, transmitted to cloud base, or absorbed by cloud column, respectively.

To measure the magnitude of horizontal fluxes, we will use the norm,

$$\|F\| = [\int_0^L |F(x)|^2 \, dx]^{1/2} \tag{5}$$

where L is the outer scale or the size of the basic cloud cell. It follows from Eq. (3) and the norm definition (5) that

$$\|H\| \le \|H_R\| + \|H_T\| + \|H_A\|. \tag{6}$$

Next we discuss the dependence of each component in Eq. (3) on single-scattering albedo, ϖ_0, and examine whether or not the magnitude of horizontal fluxes is related to radiative smoothing (Marshak et al., 1995a) and the accuracy of IPA. We will also examine how close the left and right parts of (6) are for two different solar angles.

4. Dependence on Single-Scattering Albedo

4.1 IPA accuracy on a per-pixel basis

Let us "coarse-grain" the above horizontal fluxes (H, H_R, H_T and H_A) to scale r,

$$F(r,x) = \frac{1}{r} \int_x^{x+r} F(x') \, dx' \quad (0 \le x \le L-r, \, 0 < r \le L). \tag{7}$$

It is natural to assume that if scale r in Eq. (7) grows, the assumptions of IPA become more justified, the IPA itself more accurate, and the horizontal fluxes $\|H_F(r)\|$ smaller. Figures 1a, 1b, and 1c show that this is true for H_R, H_T and H_A, i.e.,

$$\|H_F(r)\| \to 0, \; r \to L; \;\; F = R, \, T, \text{ and } A. \tag{8}$$

It follows from inequality (6) that (8) is valid for H as well. The effect of single-scattering albedo ϖ_0 on horizontal fluxes is, however, different for reflected, transmitted and absorbed photons.

Figure 1a illustrates the dependence of H_R on both r and ϖ_0. We see that the more absorption the shorter photon horizontal transport for reflected photons. As a result, the IPA pixel-by-pixel error decreases with the decrease of ϖ_0. Note that, for ϖ_0=0.9, IPA is almost accurate even on a per-pixel basis (Marshak et al., 1995b). This is expected since the contribution of multiple scattering to the albedo field decreases and very few photons travel between pixels.

The situation with transmitted photons is surprisingly different: the accuracy of the IPA on a per-pixel basis first decreases (from $\varpi_0 = 1.0$ down to $\varpi_0 = 0.98$) and only for very strongly absorbing wavelengths ($\varpi_0 > 0.98$) does it increase again (Fig. 1b) reaching the accuracy level of the conservative scattering in case of $\varpi_0 = 0.9$. To explain this, note that in contrast to standard deviation of $R_{\mathrm{IPA}}(\tau)$ which monotonically decreases with the decrease of ϖ_0 the standard deviation of $T_{\mathrm{IPA}}(\tau)$ first increases and then decreases again for strongly absorbing wavelengths. [This can be shown with a little algebra for all solar zenith angles within the 2-stream approximation (e.g., Lenoble, 1985).] A good linear relationship (not shown here) between standard deviation of $R_{\mathrm{IPA}}(\tau)$ and H_R from one side, and standard deviation of $T_{\mathrm{IPA}}(\tau)$ and H_T, from the other side, completes the explanation of both Figs. 1a and 1b.

The increase of pixel-by-pixel IPA absorption errors, $\|H_A(\varpi_0)\|$, with more absorption (Fig. 1c) is understandable; it follows directly from both the natural increase of $A_{\mathrm{IPA}}(\tau)$ itself and its standard deviation with increasing of co-albedo $1-\varpi_0$.

Figures 2a and 2b illustrate the joint effect of all horizontal fluxes [see Eq. (3)] for both high ($\theta_0 = 0^o$) and low ($\theta_0 = 60^o$) Sun. The general tendencies of horizontal fluxes are similar for both solar angles (with the increase of co-albedo, $\|H_A(\varpi_0)\|$ sharply increases, $\|H_R(\varpi_0)\|$ monotonically decreases, and $\|H_T(\varpi_0)\|$ slowly decreases for $\theta_0 = 60^o$ and first increases and then decreases for $\theta_0 = 0^o$). However, the vertically integrated ho izontal fluxes $\|H\|$ is much closer to the sum $\|H_A\|+\|H_T\|+\|H_R\|$ in case of slant illumination (Fig. 2b) than in case of zenith Sun (Fig. 2a).

To interpret this, note that for high Sun horizontal fluxes for reflected and transmitted photons are mostly anticorrelated, while for low Sun they are mostly correlated. This is a direct consequence of radiative channeling (Davis, 1992; Davis et al., 1997, 1998). As a result, for the majority of pixels the product $H_R H_T$ is negative if $\theta_0 = 0^o$ and positive if $\theta_0 = 60^o$. Thus

$$\|H\| \ll \|H_R\| + \|H_T\| + \|H_A\|, \ \theta_0 = 0^o; \tag{9a}$$

$$\|H\| \approx \|H_R\| + \|H_T\| + \|H_A\|, \ \theta_0 = 60^o, \tag{9b}$$

as we see in Figs. 2a and 2b.

Finally and most importantly, the increase in vertically integrated horizontal fluxes $\|H(\varpi_0)\|$ with the increase of co-albedo $1-\varpi_0$ is entirely determined by the increase of $\|H_A(\varpi_0)\|$. In the case of slant illumination, this is true for all single-scattering albedos while in case of high Sun only for strongly absorbing wavelengths. To conclude, horizontal flux $H(x)$ defined in Eq. (2) is not directly related to IPA accuracy for either reflectance or transmittance; for strongly absorbing wavelengths, the IPA errors $H_R(x)$ and $H_T(x)$ can be sufficiently small but nevertheless horizontal fluxes $H(x)$ are large because of the absorptance error $H_A(x)$.

An original explanation of the increase of vertically integrated horizontal fluxes with co-albedo was advanced by Titov (1998). He stated that, only in case of conservative scattering, photons traveling between neighboring pixels do not contribute to the increase of horizontal fluxes; in absorbing cases, a photon traveling back and forth horizontally changes its "weight" after each order of scattering. As a result, the more absorption, the larger changes in photon's weight, the bigger its contribution to horizontal fluxes.

4.2 Radiative smoothing and horizontal fluxes

In the case of conservative scattering, Marshak et al. (1995a) defined radiative smoothing as a radiative transfer process that diminishes the small-scale fluctuations of cloud structure producing much smoother (sometimes almost everywhere differentiable) radiation fields. Radiative smoothing is a consequence of horizontal fluxes that are driven by the gradient in cloud structure .

The scale η that characterizes this process is called "radiative smoothing scale." Based on the diffusion theory, Marshak et al. (1995a) estimated η as

$$\eta \approx \begin{cases} \langle h \rangle [(1-g)\langle \tau \rangle]^{-1/2}, & \text{for reflected radiation} \\ \langle h \rangle, & \text{for transmitted radiation} \end{cases} \quad (10)$$

Here $\langle h \rangle$ and $\langle \tau \rangle$ are the cloud's mean geometrical and mean optical thicknesses, respectively and g is the scattering phase function asymmetry factor. Davis et al. (1997b) show that the estimation (10) agrees (at least for reflected radiation) with the spatial correlations observed in Landsat scenes of marine stratocumulus by Cahalan and Snider (1989).

As was noticed earlier (Marshak et al., 1995a; Davis et al., 1997a, b), the radiative smoothing scale η serves as a critical value where IPA effectively breaks down: for scales smaller than η, real radiation fields are much smoother than their IPA counterparts which have a similar variability to cloud structure. Since the radiative smoothing scale also "measures" the scale where horizontal fluxes become important, there are two important questions to ask: How well does η characterize the magnitude of vertically integrated horizontal fluxes H and how is it related to the pixel-by-pixel IPA errors, H_F defined in Eqs. (3) and (4)?

To answer these questions we consider the effect of different single-scattering albedos ϖ_0 on the radiative smoothing scale η. Figures 3a and 3b illustrate wavenumber spectra $E(k)$ of the nadir radiance fields for three different $\varpi_0 = 0.999, 0.98, 0.95$ and two solar zenith angles $\theta_0 = 0^o$ (Fig. 3a) and $\theta_0 = 60^o$ (Fig. 3b). Both IPA and MC spectra are plotted. We start with the simplest case of Sun in zenith.

First, we see that all three IPA reflection fields have scale-invariant wavenumber spectra,

$$E(k) \sim 1/k^{\beta} \quad (11)$$

with $\beta \approx 1.5$, similar to the cloud optical depth field (see Fig. 3c). In contrast, all three MC fields exhibit a scale break that is determined by the radiative smoothing scale η and is a direct indicator of photon horizontal transport. Next, the scale break moves towards smaller scales with the decrease of ϖ_0, i.e.,

$$\eta(\varpi_0) > \eta(\varpi_0'), \text{ if } \varpi_0 > \varpi_0', \tag{12}$$

where $\eta(\varpi_0=1)$ is estimated by Eq. (10). In other words, inequality (12) states that the more absorption the smaller η; this is understandable if the rescaled optical depth in case for conservative scattering $(1-g)\langle\tau\rangle$ [see Eq. (10)] is substituted with $(1-\varpi_0 g)\langle\tau\rangle$ for absorbing wavelength (van de Hulst, 1980, Platnick, 1997).

Finally, we note in Fig. 3a that the smaller η the flatter the small-scale slope; this means less radiative smoothing, thus more accuracy in the IPA reflection. This is in good agreement with the conclusion of the last section and Fig. 1a: the pixel-by-pixel IPA error in the reflected radiation monotonically decreases with ϖ_0. From the other hand, the vertically integrated horizontal fluxes H defined in Eq. (2) increase while the horizontal fluxes for reflected photons H_R defined in Eqs. (3)-(4) decrease. Therefore, horizontal fluxes H are determined for strongly absorbing wavelengths mostly by the IPA absorption error H_A and are not directly related to the radiative smoothing scale η which relates to H_R, at least for zenith Sun.

The situation with oblique illumination (Fig. 3b) is more complex. As a direct consequence of optical shadowing, the MC reflection fields have much more fluctuations at intermediate scales than their IPA counterparts (Marshak et al., 1997). The small-scale behavior is still governed by radiative smoothing, but this is not clearly seen in the wavenumber spectra. In summary, there are two competing processes that determine the wavenumber spectra: shadowing (or "roughening") and smoothing. While the former one flattens the spectra, the later steepens it; roughening is more pronounced for intermediate scales while smoothing for small scales.

Finally, Fig. 3c illustrates wavenumber spectra for the high Sun radiation transmitted through clouds. As we see, the inequality (12) is not valid anymore. Indeed, comparing Fig. 3c with Fig. 2a, we find that scale break and the radiative smoothing scale η is determined by the horizontal fluxes for transmitted photons H_T which does not show much variability with respect to ϖ_0 (Figs. 1b and 2a). Another indication of weak dependence of η on ϖ_0 is Eq. (10) for transmitted radiation: it depends only on mean cloud geometrical thickness $\langle h\rangle$. Hence, similar to reflected fields, radiation transmitted through clouds exhibits a scale-break which is characterized

by the radiative smoothing scale η and depends only on the IPA accuracy for transmittance H_T and not on vertically integrated horizontal fluxes H.

Similar to Fig. 3c, wavenumber spectra for the radiation transmitted through clouds from the low Sun (not shown here) does not exhibit a strong ϖ_0-dependence. Because of longer photon path, the small-scale behavior of transmittance for oblique illumination is smoother than in case of zenith Sun. In contrast to up-welling radiation (Fig. 3b), the shadowing effect is well seen only for gappy clouds. Note that because of shadowing for oblique illumination, it is very hard to estimate from wavenumber spectra the smoothing effect of horizontal fluxes and IPA accuracy. This statement is valid for both up- and down-welling radiation.

5. Summary and Discussion

Vertically integrated horizontal fluxes, defined as the difference between "true" and "apparent" (measured) absorption in Eq. (2), can be represented as the sum of three "horizontal fluxes" for reflected, transmitted and absorbed photons [see Eq. (3)]. These fluxes are also pixel-by-pixel IPA errors for reflectance, transmittance and absorptance, respectively.

We show that, in general, the magnitude of vertically integrated horizontal fluxes H increase with the increase of single scattering co-albedo $1-\varpi_0$; this is true for all ϖ_0 in case of low Sun and for strongly absorbing wavelengths ($1-\varpi_0 > 0.01$) in case of high Sun. However, the increase of their magnitudes is not correlated with the accuracy of IPA for reflectance and transmittance. The accuracy of IPA on a pixel-by-pixel basis for radiation reflected from and transmitted through cloud is described by the net horizontal transport of reflected (H_R) or transmitted (H_T) photons, respectively; both are just components of the vertically integrated horizontal fluxes H. In contrast to H, the magnitude of H_R and H_T decreases with the decrease of ϖ_0 (H_R for all solar angles and H_T for low Sun) or weakly sensitive to ϖ_0 (H_T for high Sun), while the increase of vertically integrated horizontal fluxes H is due to the increase in the error of IPA absorption on a pixel-by-pixel basis.

The radiative smoothing scale η, different for reflected and transmitted radiation [see Eq. (10) and Figs. 3a and 3c), is a measure of the pixel-by-pixel accuracy of IPA. At least for high Sun and reflected radiation (Fig. 3a), η decreases with more absorption [see inequality (12)]. This effect is more hidden for low Sun because of shadowing and thus roughening at intermediate scales (Fig. 3b). For transmitted photons, η remains almost insensitive to the changes in ϖ_0 (Figs. 2a, 2b and 3c).

The results summarized above are robust. Indeed, the same tendencies in horizontal fluxes are observed in 2D vs. 1D horizontal variabilities, in presence vs. absence of vertical inhomogeneity, in variable vs. flat cloud top and base, with strong surface albedo vs. a "black" surface, and, finally, with Henyey-Greenstein vs. realistic phase function with the same asymmetry parameter. Of course, the magnitude of horizontal fluxes increases with the gradients in cloud structure. Stronger cloud variability, clear sky gaps in cloud structure and oblique illumination may substantially enhance the magnitude of horizontal fluxes as additional sources for photon horizontal transport. All these factors make the situation very complex and often when analyzing high resolution satellite images one cannot distinguish between the competing effects of radiative smoothing and geometrical shadowing for both transparent and absorbing channels.

Acknowledgments

This work was supported by the Environmental Sciences Division of U.S. Department of Energy (under grant DE-A105-90ER61069 to NASA's Goddard Space Flight Center) as part of the Atmospheric Radiation Measurement (ARM) program, and by NASA's EOS Project Science Office at Goddard Space Flight Center (under grant NAG5-6675) as part of the EOS Validation Program. We thank Dr. David Starr, as EOS Validation Scientist, for the support of this project. We thank R. Cahalan, R. Pincus, S. Platnick, and G. Titov for stimulating discussions.

References

Ackerman, S. A., and S. K. Cox, 1981: Aircraft observations of the shortwave fractional absorptance of non-homogeneous clouds. *J. Appl. Meteor.*, **20**, 1510–1515.

Barker, H. W., 1996: Estimating cloud field albedo using one-dimensional series of optical depth. *J. Atmos. Sci.*, **53**, 2826–2837.

Cahalan, R. F., and J. B. Snider, 1989: Marine stratocumulus structure during FIRE. *Remote Sens. Environ.*, **28**, 95–107.

Cahalan, R. F., 1994: Bounded cascade clouds: Albedo and effective thickness. *Nonlinear Processes in Geoph.*, **1**, 156–167.

Cahalan, R. F., W. Ridgway, W. J. Wiscombe, T. L. Bell, and J. B. Snider, 1994: The albedo of fractal stratocumulus clouds. *J. Atmos. Sci.*, **51**, 2434–2455.

Cess, R. D., M. Zhang, P. Minnis, L. Corsetti, E. G. Dutton, B. W. Forgan, D. P. Garber, W. L. Gates, J. J. Hack, E. F. Harrison, X. Jing, J. T. Keihl, C. N. Long, J.-J. Morcrette, G. L. Potter, V. Ramanathan, B. Subasilar, C. H. Whitelock, D. F. Young, and Y. Zhou, 1995: Absorption of solar radiation by clouds: observations versus models. *Science*, **267**, 496–499.

Chambers, L., B. Wielicki, and K. F. Evans, 1997: On the accuracy of the independent pixel approximation for satellite estimates of oceanic boundary layer cloud optical depth. *J. Geophys. Res.*, **102**, 1779–1794.

Davis, A., 1992: *Radiation Transport in Scale-Invariant Optical Media.* Ph.D. Thesis, McGill University, Physics Department, Montreal (Qc).

Davis, A., A. Marshak, W. J. Wiscombe, and R. F. Cahalan, 1997a: Evidence for net horizontal radiative fluxes in marine stratocumulus. In *IRS'96: Current Problems in Atmospheric Radiation*, Eds. W. L. Smith and K. Stamnes, Deepak Publ., Hampton (Va), pp. 809–812.

Davis, A., A. Marshak, R. Cahalan, and W. Wiscombe, 1997b: The LANDSAT scale-break in stratocumulus as a three-dimensional radiative transfer effect, implications for cloud remote sensing. *J. Atmos. Sci.*, **54**, 241–260.

Davis, A., A. Marshak, R. F. Cahalan, and W. J. Wiscombe, 1997c: Interactions: Solar and Laser Beams in Stratus Clouds, Fractals & Multifractals in Climate & Remote-Sensing Studies. *Fractals*, **5**, 129-166.

Davis, A., A. Marshak, R. F. Cahalan, and W. J. Wiscombe, 1998: Insight into three-dimensional radiation transport processes from diffusion theory, with applications to the atmosphere. In *Proceedings of International Symposium on Radiative Transfer*, 1997, Eds. P. Mencuc and F. Arinc, Begell House Publ., New York (NY), in press.

Deirmendjian, D., 1969: *Electromagnetic Scattering on Spherical Polydispersions.* Elsevier, New York (NY), 292 pp.

Lenoble, J. (Ed.), 1985: *Radiative Transfer in Scattering and Absorbing Atmospheres: Standard Computational Procedures*, 300 pp., Deepak Publ., Hampton (Va).

Mandelbrot, B. B., 1977: *Fractals: Form, Chance, and Dimension*, 365 pp., W. H. Freeman, San Francisco (Ca).

Marchuk, G., G. Mikhailov, M. Nazaraliev, R. Darbinjan, B. Kargin, and B. Elepov, 1980: *The Monte Carlo Methods in Atmospheric Optics*, 208 pp., Springer-Verlag, New-York (NY).

Marshak, A., A. Davis, R. F. Cahalan, and W. J. Wiscombe, 1994: Bounded cascade models as non-stationary multifractals. *Phys. Rev. E*, **49**, 55–69.

Marshak, A., A. Davis, W. Wiscombe, and R. Cahalan, 1995a: Radiative smoothing in fractal clouds. *J. Geophys. Res.*, **100**, 26247–26261.

Marshak, A., A. Davis, W. Wiscombe, and G. Titov, 1995b: The verisimilitude of the independent pixel approximation used in cloud remote sensing. *Remote Sens. Environ.*, **52**, 72–78.

Marshak, A., A. Davis, W. Wiscombe, and R. Cahalan, 1997: Inhomogeneity effects on cloud shortwave absorption measurements: Two-aircraft simulations. *J. Geophys. Res.*, **102**, 16619–16637.

Marshak, A., A. Davis, W. J. Wiscombe, W. Ridgway, and R. F. Cahalan, 1998: Biases in shortwave column absorption in the presence of fractal clouds. *J. Climate*, **11**, 431–446.

Min, Q. L., and L. C. Harrison, 1996: Cloud properties derived from surface MFRSR measurements and comparison with GOES results at the ARM SGP site. *Geophys. Res. Lett.*, **23**, 1641–1644.

Pincus, R., M. D. King, S. Platnick, and S.–C. Tsay, 1997: *In situ* measurements of the absorption of solar radiation in stratiform water clouds. In *IRS'96: Current Problems in Atmospheric Radiation*, Eds. W. L. Smith and K. Stamnes, Deepak Publ., Hampton (Va), pp. 197–200.

Platnick S., 1997: The scales of photon transport in cloud remote sensing problems. In *IRS'96: Current Problems in Atmospheric Radiation*, Eds. W. L. Smith and K. Stamnes, Deepak Publ., Hampton (Va), pp. 206–209.

Stamnes, K., S.–C. Tsay, W. J. Wiscombe and K. Jayaweera, 1988: Numerically stable algorithm for discrete-ordinate-method radiative transfer in multiple scattering and emitting layered media. *Appl. Opt.*, **27**, 2502–2512.

Titov, G. A. and E. I. Kasjanov, 1997: Radiative Effects of Inhomogeneous Stratocumulus Clouds. In *IRS'96: Current Problems in Atmospheric Radiation*, Eds. W. L. Smith and K. Stamnes, Deepak Publ., Hampton (Va), pp. 78–81.

Titov, G. A., 1998: Radiative horizontal transport and absorption in stratocumulus clouds. *J. Atmos. Sci.*, **55**, 2549–2560.

Van de Hulst, H. C., 1980: *Multiple Light Scattering: Table, Formulas, and Applications*. 2 Vols., Academic Press, San Diego (Ca).

Wiscombe, W. J., 1995: An absorption mystery. *Nature*, **376**, 466-467.

Zuidema P. and K. F. Evans, 1998. On the validity of the Independent Pixel Approximation for the boundary layer clouds observed during ASTEX. *J. Geophys. Res.*, **103**, 6059–6074.

FIGURE CAPTIONS

Figure 1: *Dependence of pixel-by-pixel IPA accuracy* $\|H_F\|$ *on averaging scale r and single-scattering albedo* ϖ_0. Horizontal distribution of cloud optical depth is simulated with bounded cascade models (p = 0.3, H = 1/3, $\langle\tau\rangle$ = 13, 10 cascades, pixel size = 25 m). Flat cloud top and cloud base, geometrical thickness h = 300 m. No cloud gaps are added. Henyey-Greenstein phase functions with asymmetry parameter g = 0.85 is used. Surface is "black." The results are averaged over ten independent realizations. Solar zenith angle θ_0=0°, single-scattering albedo ϖ_0 = 1.0, 0.999, 0.99, 0.98, 0.95, 0.9. **(a)** Reflectance, $\|H_R\|$; **(b)** Transmittance, $\|H_T\|$; **(c)** Absorptance, $\|H_A\|$.

Figure 2: *Pixel-by-pixel IPA accuracy for reflectance, transmittance, absorptance, their sum, and the total horizontal fluxes H.* Cloud model and scattering conditions are the same as in Fig. 1. **(a)** θ_0=0°; **(b)** θ_0=60°.

Figure 3: *Wavenumber spectra E(k) for the IPA and MC calculated radiation fields.* Cloud model and scattering conditions are the same as in Fig. 1. Three single-scattering albedos ϖ_0 are used: 0.999, 0.98, and 0.95. **(a)** θ_0=0°, nadir radiance; **(b)** θ_0=60°, nadir radiance; **(c)** θ_0=0°, transmittance (cloud optical depth is added for reference).

Fig. 1a

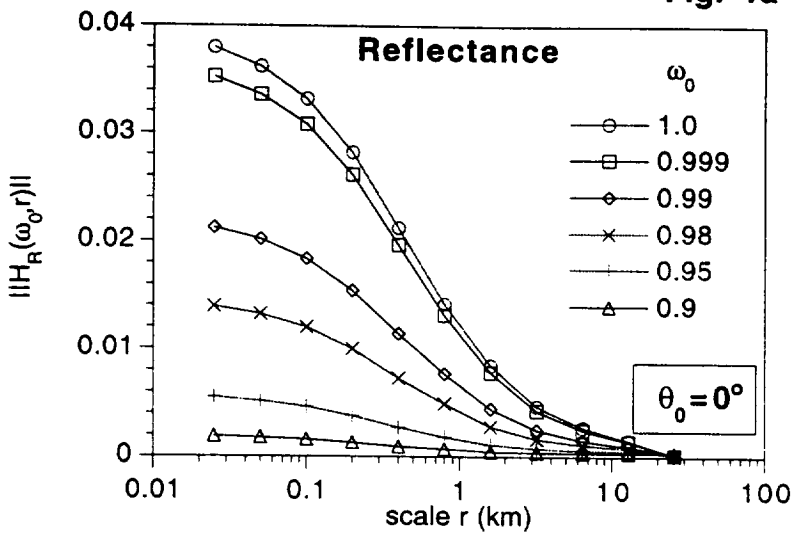

Fig. 1b

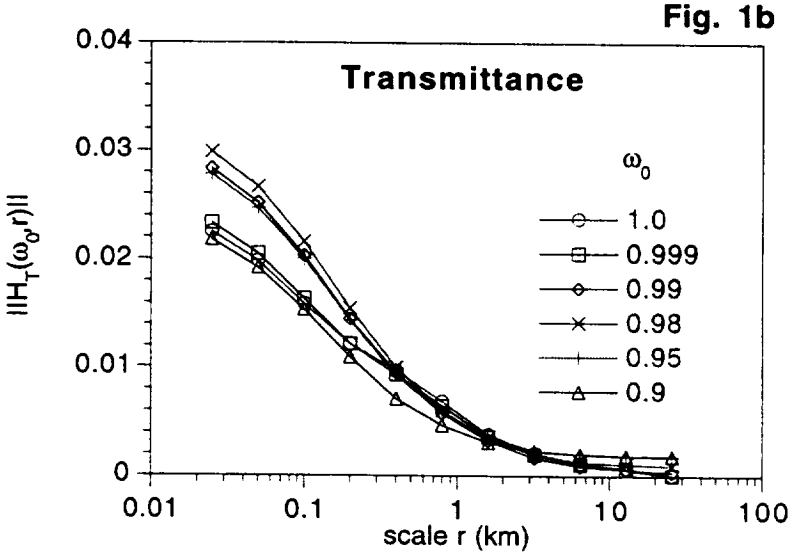

Fig. 1c

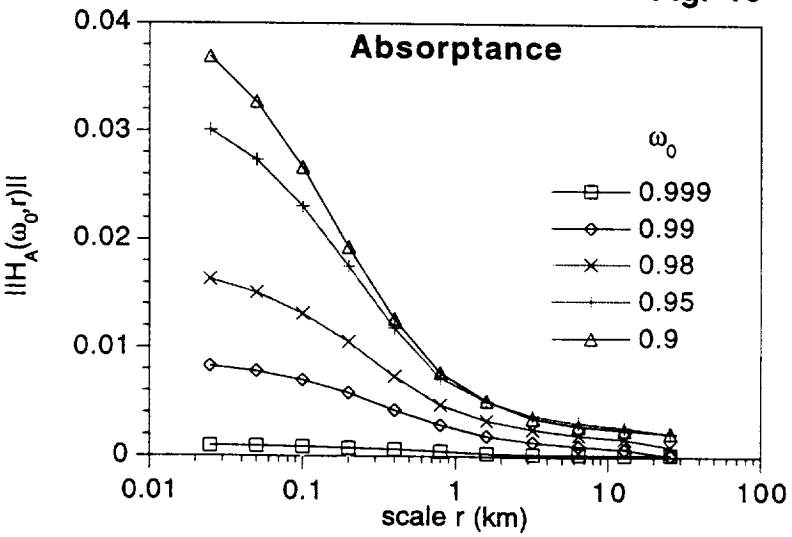

Fig. 2a

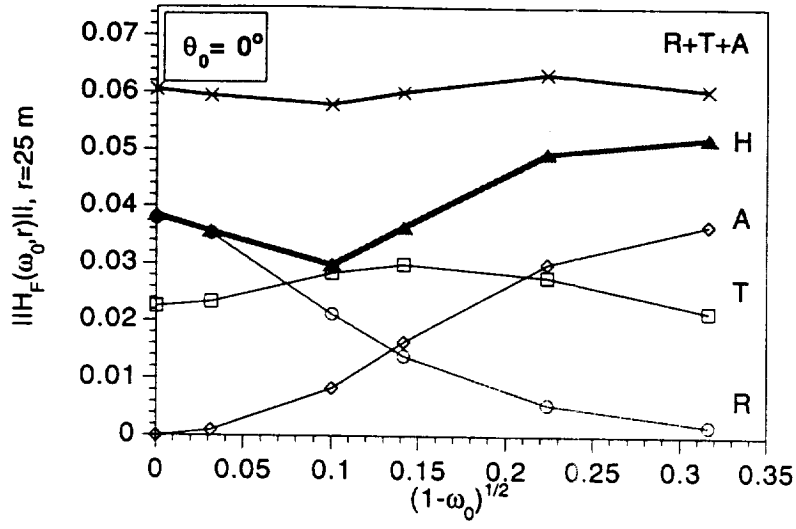
θ0= 0°
R+T+A
H
A
T
R
||HF(ω0,r)||, r=25 m
(1-ω0)1/2
0.07
0.06
0.05
0.04
0.03
0.02
0.01
0
0.05
0.1
0.15
0.2
0.25
0.3
0.35

Fig. 2b

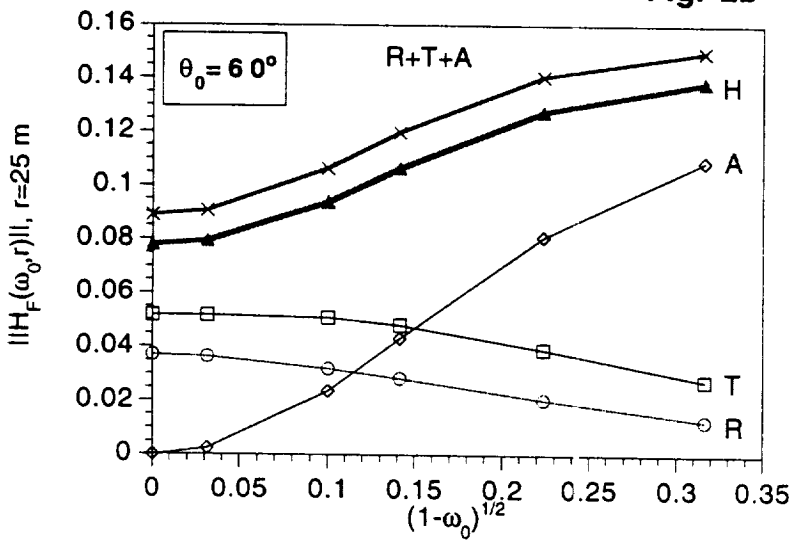
θ0= 6 0°
R+T+A
H
A
T
R
||HF(ω0,r)||, r=25 m
(1-ω0)1/2
0.16
0.14
0.12
0.1
0.08
0.06
0.04
0.02
0
0.05
0.1
0.15
0.2
0.25
0.3
0.35

Fig. 3a

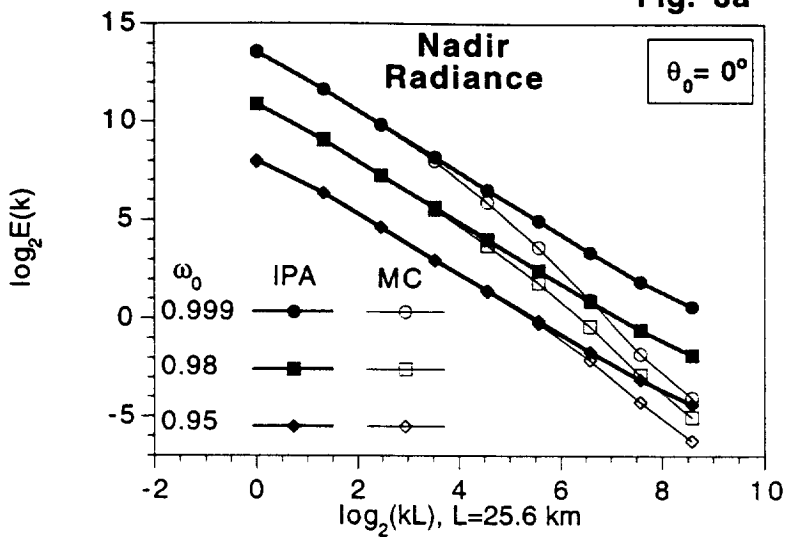

Fig. 3b

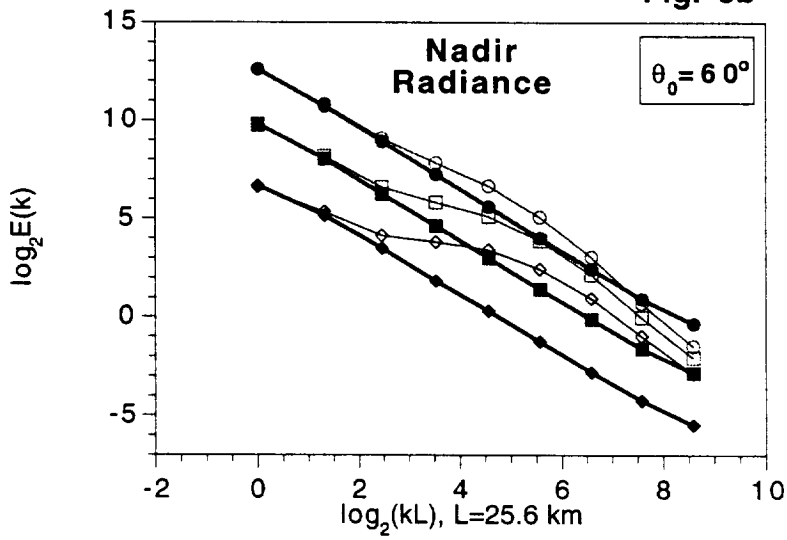

Fig. 3c